

Contact Detection and Reaction of a Wheelchair Mounted Robotic Arm Equipped with Mechanical Gravity Canceller

Wei Wang, Yuki Suga and Shigeki Sugano

Abstract—Safety issue has become the primary concern in wheelchair mounted robotic arm applications. We introduced mechanical gravity canceller in the design to realize a light weight manipulator, which also yield the greatly simplify of manipulator dynamics. Based on the simplified dynamics, sensor based contact detection can be easily implemented to enable safety. Contact reaction schemes are also applied through a impedance control law to achieve desired backdrivability. Experiments are conducted to illustrate the proposed method.

I. INTRODUCTION

Industry robots played up to now the most important role in real-world applications. However, with the theoretical progress as well as technical advances in the research field of robotics, and also the exponentially increase of computer power, it make us to believe that it is the time to develop the robots that work in the vicinity of and together with humans, for example, the assistive and rehabilitation robots that will be under great requirement in the more and more aging society to support disabled as well as elderly people during their daily life activities [1] [2]. Such robotic systems are always comparatively challenging and greatly benefit from the improvements in sensor systems and control techniques.

Wheelchair mounted robotic arm (WMRA) is one kind of assistive and rehabilitation robots that works in the close vicinity of human beings. It is developed as an assistive device, in an attempt to help elderly and disabled people to recover some manipulation capabilities in activities of daily livings (ADLs). The idea of WMRA comes from the healthcare condition survey which showed that a lot of disabled people as well as a growing number of elderly people owing to the more and more aging society, have difficulty performing functional activities and requires an assistive device to enhance their manipulation ability [3]-[6]. WMRA is a robotic solution that combines the idea of a mobile based manipulator and a powered wheelchair as the platform to mount the manipulator, several WMRA systems have been developed for use in both academic and industry society, for example, the FRIEND II and FRIEND

III projects that are under progress in University of Bremen, the commercial available arms: the Manus manufactured by Exact Dynamics, and the Raptor manufactured by Applied Resources [7]-[9]. The idea of these WMRA could provide the users with combined mobility and manipulation control, for the assistance in ADLs.

With respect to the WMRA application where the manipulator will share the environment with human and allow a close physical cooperation, safety issues becomes the primary concern. Unlike the robots in traditional industrial applications, light weight design and soft-robotic features are greatly required for the necessary level of safety to avoid the harm to humans and also the robot damage that may occur during an occasional contact. The critical importance of safety has pushed an intensive research in physical human-robot interaction, not only for the WMRA application, but also in all the domestic, entertainment, assistive, rehabilitation and medical application fields, and lead to a number of impressive realizations [10]-[13]. Series elastic actuator (ESA) is one solution of compliant actuators that introduces an instrumented elasticity between the gear trains output and the load vastly to improve the quality of the actuator package while paradoxically reducing its cost, and proved to be particularly strong for actuators intended for robots that interact with the natural environment [14] [5]. Another passive impedance control method is proposed based on mechanical impedance adjuster (MIA), in which the spring constant and damping coefficient can be changed to achieve the impedance required for a given interactive task [16]. Except for these mechanical solutions to reduce the severity of impacts passively, external sensors are also exploited to realize an active impedance control. For example, the impressive DLR lightweight robot that enables a high payload to weight ratio up to 14kg/14kg, employed a controller structure based on a feedback of the joint torques as well as the link side positions, and leads to a great performance of compliance [17] [18].

However, common drawbacks have to be taken into consideration with respect to the special WMRA application. The mechanical solutions always incorporate complicated mechanical design of compliant components, thus yield the implementation of a big and heavy manipulator that is not suitable to be mounted on a wheelchair; whereas the torque sensor based impedance control is always difficult and performance limited due to the highly varying dynamic characteristics that is difficult to follow, for example, possibly large deviations of gravity compensation may occur due to the flexibility of joints [19] [20], noise and an intrinsic

This work was supported in part by Global COE Program "Global Robot Academia" from the Ministry of Education, Culture, Sports, Science and Technology of Japan, and the WABOT HOUSE project of Gifu prefecture in Japan

W. Wang is with the Department of Modern Mechanical Engineering, School of Creative Science and Technology, Waseda University, Tokyo 169-8555, Japan wangwei@sugano.mech.waseda.ac.jp

Y. Suga, is with the Department of Modern Mechanical Engineering, School of Creative Science and Technology, Waseda University, Tokyo 169-8555, Japan ysuga@suou.waseda.jp

S. Sugano is with the Faculty of Department of Modern Mechanical Engineering, School of Creative Science and Technology, Waseda University, Tokyo 169-8555, Japan sugano@waseda.jp



Fig. 1. Light Weight Arm

delay are also introduced and are indispensable because of the numerical differentiation of velocity or position data in a digital implementation. In order to corresponding the requirement of WMRA application, we have developed a light weight manipulator equipped with mechanical gravity canceller (MGC), see Fig. 1. The MGC is design to balance the link gravity in arbitrary postures by generating the corresponding gravity compensation torque through the force of a linear torsion spring, thus benefit the WMRA application in two aspects:

(1) The cancellation of self gravity enables the realization of a lightweight design, that reduces manipulator inertia and weight

(2) The employment of MIA simplifies the dynamics of the manipulator dramatically, thus enhance the performance and reliability of torque sensor based impedance control.

In this paper, our research is mainly focus on the contact detection and reaction of a WMRA equipped with MGC, aims to achieve the soft-robotic features that is critical important for the physical human-robot interaction during the task execution of ADLs. The dynamic model of our developed light weight manipulator is investigated through the Newton Euler formulation, and was shown to be dramatically simplified due to the employment of MGC. Benefit from the simplicity of dynamics, torque sensors mounted on the base joint are easier to be utilized to generate an estimate of external torque in the pitch and yaw direction. Contact reaction strategy is also developed through an impedance control law to achieve the desired back drivability in both pitch and yaw joint.

The reminders of this paper are organized as follows: Section II provides the detailed dynamics interpretation of our light weight manipulator equipped with MGC. In section

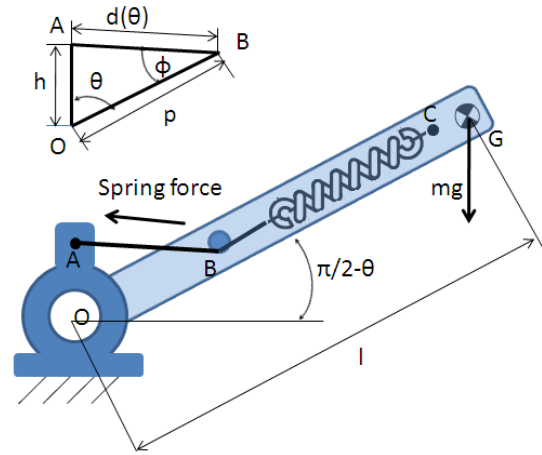


Fig. 2. Single Joint Model

III, a contact detection scheme is applied to generate an estimate of external torques in the yaw and pitch direction. Section IV introduces the contact reaction strategy that applies an impedance control law to achieve the desired back drivability. Experiment and results are described in section V, Conclusions are included in section VI.

II. DYNAMICS INTERPRETATION

A. Single Joint Model

The gravity-induced joint loads are always significant and consume a large amount of actuator torque and energy, mechanical gravity cancellation (MGC) is the mechanical solution to compensate gravitational torque, thus reduce the energy consumption of motors. Several prototypes of mechanical gravity canceller has been investigated [21] [22]. The basic idea generally implicate that: through the utilization of spring elements to generate the balance torque, thus changes in potential energy associated with link motion through a gravity field can be mapped to changes in strain energy storage in spring elements.

Consider the idealized single-joint model shown in Fig. 2. The link mass m is concentrated at a distance L from the joint pivot O , a coil spring element is arranged inside the link, by connecting a wire to the fix point (Point O) of joint base through bending point (Point B). A nonlinear compensation torque will be generated by the spring force to balance the gravity induced torque. The spring torque and gravity torque is derived as:

$$\tau_{gravity} = mgl\sin(\theta) \quad (1)$$

$$\begin{aligned} \tau_{spring} &= psin(\psi)F_{spring} \\ &= p\frac{hsin(\theta)}{d(\theta)}k\Delta r(\theta) \\ &= phk\frac{\Delta r(\theta)}{d(\theta)}sin(\theta) \end{aligned} \quad (2)$$

where k is the spring constant, $\Delta r(\theta)$ is the displacement of the spring element from its natural length.

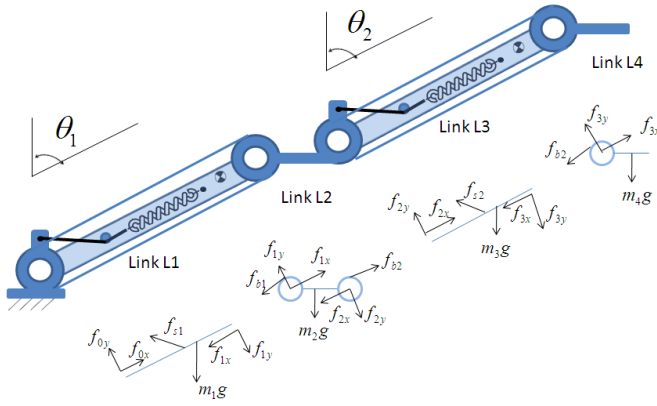


Fig. 3. Two DOF Model

Ideally, the gravity compensation will be achieved when τ_{spring} equals $\tau_{gravity}$, and we can derive:

$$phk \frac{\Delta r(\theta)}{d(\theta)} \sin(\theta) = mgl \sin(\theta) \quad (3)$$

In order to balance the gravity induced torque in arbitrary postures, the θ terms have to be eliminated in equation (3), thus requires the term $\frac{\Delta r(\theta)}{d(\theta)}$ to be independent of θ .

In fact, it is the nonlinearity of $\frac{\Delta r(\theta)}{d(\theta)}$ that makes it difficult to generate accurate compensation torque. However, through a special geometrical arrangement of the spring element and cable, the term $\Delta r(\theta) = d(\theta)$ will be satisfied. This geometrical arrangement implicate that: the length from point C to bending point B equals the sum of cable length and spring natural length. When the link is in the vertical posture, it also can be interpreted as that: the spring displacement $\Delta r(0)$ generated in the vertical posture equals the length from point A to point B.

Under the condition that $\Delta r(\theta) = d(\theta)$ is satisfied, the appropriate spring constant is computed according to (3):

$$k = \frac{mgl}{ph} \quad (4)$$

Thus k is utilized for the selection of appropriate spring element to balance the gravity induced torque.

B. Two DOF Arm Model

When we incorporate the mechanical gravity compensation mechanism into the design of a robotic arm which always has more than one link, the variation of gravity induced torque generated by the posture change of the next link has to be taken into consideration. Generally, the gravity torque variation is always complicated with its nonlinearity and difficult to follow. It is more feasible if we utilize a special mechanism to decompose the gravity torque in base joint from the posture change of the next link.

We adopt a parallelogram mechanism which utilizes two pulleys connected with a belt, as depicted in Fig. 3. The link L2 is kept in the constant posture during the rotation of link L1, due to the constraint generated by the belt force. We use the NewtonEuler formulation to analysis the dynamics of a

2 DOF arm model. The forces acting on each link are shown in Fig. 3.

Herein, m_1, m_2, m_3, m_4 are the mass of each link, θ_1 and θ_2 are the angle of two revolute joints, $f_{0x}, f_{0y}, f_{1x}, f_{1y}, f_{2x}, f_{2y}, f_{3x}, f_{3y}$ denote the reaction forces of neighboring links in the parallel and perpendicular directions with respect to the link, f_{b1}, f_{b2} are the belt forces, f_{s1}, f_{s2} are the forces exerted by the spring.

Firstly, the static force balance equation of link L4 is obtained as:

$$f_{3y} = m_4 g \sin(\theta_2) \quad (5)$$

(5) represents the variation of gravity effect induced by the neighboring link, thus the gravity compensation equation of link L3 can be remodeled as:

$$\begin{aligned} \tau_{spring} &= \tau_{gravity} \\ &= m_3 g l_{o3} \sin(\theta_2) + m_4 g l_3 \sin(\theta_2) \\ &= (m_3 g l_{o3} + m_4 g l_3) \sin(\theta_2) \end{aligned} \quad (6)$$

where l_3 denotes the length of Link3, l_{o3} denotes the length between gravity point of Link3 to the revolute point of joint 2.

The refined term of $\tau_{gravity}$ is still a linear function of $\sin(\theta_2)$, thus we only need to re-compute k of the spring element to balance the overall gravity induced torque.

When the motor torque and external torque are applied, we can obtain the dynamics of link L3 and link L4 driven by the revolute joint 2 as follows:

$$\begin{aligned} \tau_{m2} &= \tau_{spring} - \tau_{gravity} + (I_{34})\ddot{\theta}_2 - \tau_{ext} \\ &= phk \sin(\theta_2) - (m_3 g l_{o3} + m_4 g l_3) \sin(\theta_2) \\ &\quad + (I_{34})\ddot{\theta}_2 - \tau_{ext} \\ &= (I_{34})\ddot{\theta}_2 - \tau_{ext} \end{aligned} \quad (7)$$

where τ_{m2}, τ_{ext} denotes the motor torque and external torque applied, I_{34} is the moment of inertia.

If we regard link L2, L3, L4 as a whole rigid body, the dynamics of revolute joint 1 can be obtained in the same way:

$$\tau_{m1} = (I)\ddot{\theta}_1 - \tau_{ext} \quad (8)$$

With respect to our developed light weight arm, there are 4 degree of freedom, 2 dof is with the pitch joint motion that was described above, whereas the other 2 dof belongs to the yaw joint motion that has no relation with gravity effect. The yaw joint motion and pitch joint motion will be handled separately in the following sections.

III. CONTACT DETECTION

Contact detection generally implicate the detection and estimation of an external force or its resulting torque that may applied at any locations along the robot arm. It acts as the first and most important step for the physical human



Fig. 4. Wheelchair Mounted Robotic Arm

robot interaction. With respect to our 4 DOF light weight robot arm, two torque sensors are employed in base joints to measure motor torques for the estimation of external torques applied in the yaw and pitch directions, see Fig. 4. We use $\theta_1, \theta_2, \theta_3, \theta_4$ to denote the joint variables, with θ_1 and θ_3 related to the yaw direction motion, and θ_2 and θ_4 related to the pitch direction motion,

The dynamics of the pitch joint can be modeled from (8) when an external torque is applied. In order to obtain higher practical performance, the gravity compensation error should be considered as well as the viscoelasticity of joint. Actually we adopted capacitance torque sensor as well as gear head instead of harmonic drive to reduce the elasticity of joint, thus we model the viscoelastic joint as a damping joint.

$$\tau_m^p = I^p \ddot{\theta}_2 + D^p \dot{\theta}_2 - g(\theta_2) - \tau_{ext}^p \quad (9)$$

$$\tau_s^p = \tau_m^p \quad (10)$$

where $\tau_m^p, I^p, D^p, \tau_{ext}^p, \tau_s^p$ denotes motor torque, moment of inertia, damping factor, external torque, torque measure of sensor in the pitch direction respectively, $g(\theta_2)$ is the gravity compensation error which can be find as a nonlinear function of the pitch joint angle θ_2 .

The dynamics of the yaw joint motion has no relationship with the gravity effect, as can be obtained:

$$\tau_m^y = I^y \ddot{\theta}_1 + D^y \dot{\theta}_1 + I_c^y \ddot{\theta}_3 + D_c^y \dot{\theta}_3 - \tau_{ext}^y \quad (11)$$

$$\tau_s^y = \tau_m^y \quad (12)$$

where $\tau_m^y, I^y, D^y, \tau_{ext}^y, \tau_s^y$ denotes motor torque, moment of inertia, damping factor, external torque, torque measure of

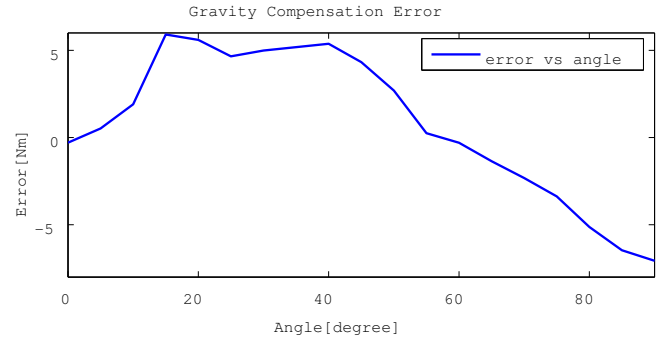


Fig. 5. Gravity Compensation Error

sensor in the yaw motion direction respectively, $(I_a^y) \ddot{\theta}_3 + D_a^y \dot{\theta}_3$ represent the coupling torque generated by the yaw motion of θ_3 .

From a theoretical point of view, contact detection well defines a disturbance estimation problem which must be solved to generate an estimate of the external torque $\tau_{ext}^p, \tau_{ext}^y$ regarded as system disturbance, through the utilization of torque sensor measure τ_s^p, τ_s^y and joint variable $\theta_1, \theta_2, \theta_3, \theta_4$. Benefits from the simplicity of dynamics, the gravity compensation error and inertia term can be identified and computed separately thus ease the estimation process.

A. Gravity Compensation Error

Gravity compensation error occurs due to the fact that it is impossible to select a spring element with spring constant equals the computed value, the nonlinear spring characteristic and computation error also has a big influence. We conducted an experiment to obtain gravity compensation error with respect to the pitch joint variable θ_2 , as can be depicted in Fig. 5.

The gravity compensation error can be regarded as a nonlinear function of θ_2 , thus we use a interpolated lookup table to model the nonlinearity. The lookup table is then utilized in real-time application.

B. Inertia and Damping Terms

A parameter identification experiment is also conducted to compute the moment of inertia and damping factor.

At the first identification step, the pitch joint rotates at a constant velocity $\dot{\theta}_2$ when the acceleration $\ddot{\theta}_2$ is found to be zero, thus the measured data of $\theta_2, \dot{\theta}_2, \tau_s^p$ are used to numerically compute the damping factor D^p through a standard least square method. The computed D^p is then used in the second identification step to compute the moment of inertia I^p .

At the second identification step, the pitch joint accelerate to a constant speed, the data $\tau_s^p, \theta_2, \dot{\theta}_2, \ddot{\theta}_2$ acquired during the acceleration can be easily used to compute the moment inertia I^p .

The identification method can be used similarly in the yaw joint to compute its damping and inertia factor.

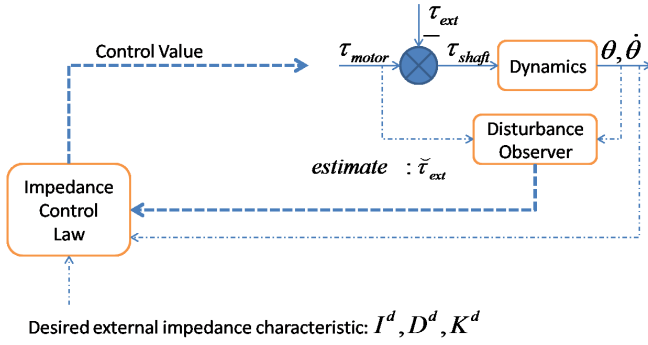


Fig. 6. Control Architecture

C. Estimate of External Torque

Based on the identified damping and inertia factor, as well as the gravity compensation error modeled, we can formulate our disturbance observer to obtain the estimate of external torque as follows:

$$\hat{\tau}_{ext}^p = I^p \ddot{\theta}_2 + D^p \dot{\theta}_2 - g(\theta_2) - \tau_s^p \quad (13)$$

$$\hat{\tau}_{ext}^y = I^y \ddot{\theta}_1 + D^y \dot{\theta}_1 + I_c^y \ddot{\theta}_3 + D_c^y \dot{\theta}_3 - \tau_s^y \quad (14)$$

where $\hat{\tau}_{ext}^p, \hat{\tau}_{ext}^y$, denotes the estimated external torque applied in the pitch and yaw direction respectively.

IV. CONTACT REACTION

When a contact occurrence is detected, the controller should then switch to an appropriate reaction strategy to avoid possible physical damage. A simple example is to stop the robot when the external torque detected exceeds a threshold. However, it is not suitable when there are active contacts.

We employed impedance control in our contact reaction scheme aims at the achievement of a desired dynamical relation between external forces and robot movement. The concept of "External Impedance" is introduced to describe the desired dynamic characteristic with respect to applied external torque. When the external torque estimated in the contact detection exceeds a threshold, the impedance law will be activated and compute the corresponding control value based on the feedback of estimated external torque to achieve the desired External Impedance. The control architecture is shown in Fig. 6.

Consider the dynamic model shown in (9) and (10), if we apply the impedance control law as follows:

$$\tau_m^p = K \tau_{ext}^p + P(\theta_2 - \theta_2^d) + D \dot{\theta}_2 - g(\theta_2) \quad (15)$$

where K denotes gain of external torque feedback, P, D is position and velocity gain, θ_2^d is the equilibrium position when the external torque is removed. The closed loop dynamics is formulated as:

$$(K+1)\tau_{ext}^p = I^p \ddot{\theta}_2 + (D^p - D)\dot{\theta}_2 + P(\theta_2 - \theta_2^d) \quad (16)$$

$$\tau_{ext}^p = \frac{I^p}{K+1} \ddot{e} + \frac{(D^p - D)}{K+1} \dot{e} + \frac{P}{K+1} e \quad (17)$$

Where $e = \theta_2 - \theta_2^d$. Herein, the closed loop system was found to be a two order system, with the inertia $\frac{I^p}{K+1}$, damping $\frac{(D^p - D)}{K+1}$, and stiffness $\frac{P}{K+1}$. In order to achieve the desired "external impedance" described with stiffness K^d , damping D^d , and inertia I^d , it requires:

$$I^d = \frac{I^p}{K+1} \quad (18)$$

$$D^d = \frac{(D^p - D)}{K+1} \quad (19)$$

$$K^d = \frac{P}{K+1} \quad (20)$$

Thus, the gains of impedance control law are obtained as:

$$K = \frac{I^p}{I^d} - 1 \quad (21)$$

$$D = D^p - (K+1)D^d \quad (22)$$

$$P = (K+1)K^d \quad (23)$$

From the above equations, we can formulate our impedance control law shown in (15). In order to design an effective impedance controller, a very important step should be the determination of desired "External impedance" described with stiffness K^d , damping D^d , and inertia I^d . Generally "External impedance" could be related with soft-robotic feature of robots that has revealed its great important in the physical human robot interaction applications, low stiffness always represent that the robot is much softer, while good backdrivability requires lower damping and inertia. The physical interpretation is also helpful in the selection of "External impedance".

V. EXPERIMENTS

Experiments are conducted to verify the proposed contact detection and reaction scheme. The hardware platform is our developed wheelchair mount robotic arm equipped with mechanical gravity canceller.

In order to test the contact detection scheme, an external torque generated by humans was applied on the robot in the direction of pitch joint movement. The estimated external torque and also the motor torque measured by torque sensor and are shown in Fig. 7. We use a contact threshold to detect the occurrence of an external contact, the rectangle area in Fig. 7 denotes the contact period.

In the test of contact reaction scheme, the impedance control law will be activated during the detected contact period, thus the robot will move to achieve desired dynamic characteristic with respect to the estimated external torque. The joint movement as well as external torque and motor torque are shown in Fig. 8.

VI. CONCLUSIONS AND FUTURE WORKS

Wheelchair mounted robotic arm applications require light weight arm that can also provide high level safety control. The employment of mechanical gravity canceller not only enabled a considerable light weight design through the compensation of self-gravity, but also simplified the robot dynamics greatly. Thus we could implement the sensor

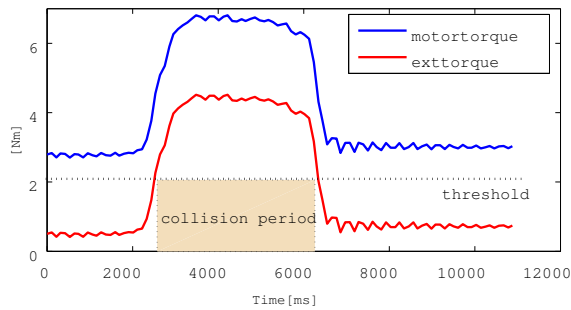


Fig. 7. Contact Detection Result

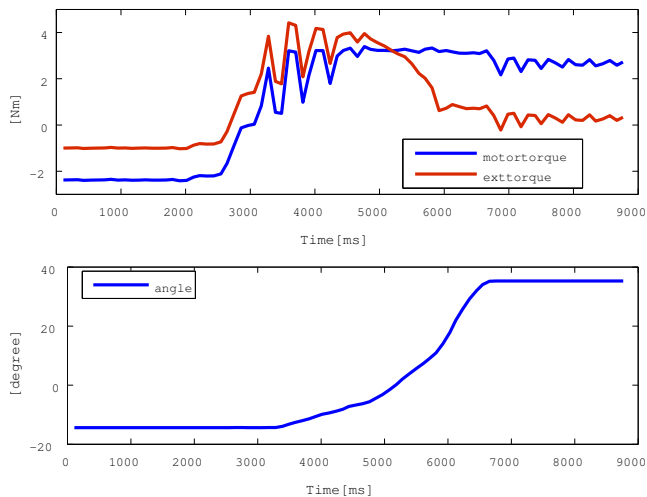


Fig. 8. Contact Reaction Result

based contact detection and reaction scheme more reliably. The contact detection scheme that generates an estimate of external torque is proposed, as well as the corresponding contact reaction strategy that utilizes an impedance control law to achieve the desired external impedance characteristic. The future work will be focused on how to incorporate the contact detection and reaction scheme into our task execution architecture of the wheelchair mounted robotic arm system.

VII. ACKNOWLEDGMENTS

This work was supported in part by Global COE Program "Global Robot Academia" from the Ministry of Education, Culture, Sports, Science and Technology of Japan, and the WABOT HOUSE project of Gifu prefecture in Japan.

REFERENCES

- [1] J. F. Engelberger, *Robotics in service*. The MIT press, 1989.
- [2] C. Balaguer, A. Gimenez, A. Jardon, R. Cabas, and R. Correal, "Live experimentation of the service robot applications for elderly people care in home environments," in *2005 IEEE/RSJ International Conference on Intelligent Robots and Systems, 2005.(IROS 2005)*, 2005, pp. 2345–2350.
- [3] S. D. Prior, "An electric wheelchair mounted robotic arm—a survey of potential users," *Journal of medical engineering & technology*, vol. 14, no. 4, pp. 143–154, 1990.

- [4] C. Stanger, C. Anglin, W. Harwin, and D. Romilly, "Devices for assisting manipulation: a summary of user task priorities," *IEEE Transactions on Rehabilitation Engineering*, vol. 2, no. 4, pp. 256–265, 1994.
- [5] R. M. Alqasemi, E. J. McCaffrey, K. D. Edwards, and R. V. Dubey, "Analysis, evaluation and development of wheelchair-mounted robotic arms," in *IEEE Int. Conf. on Rehabilitation Robotics*, 2005, p. 469472.
- [6] G. Rmer, A. Peters, E. Koerhuis, and H. Stuyt, "Assistive robotic manipulator (arm)-cost-savings and economic benefits," *International Journal of Assistive Robotics and Mechatronics*, vol. 7, no. 2, pp. 20–25, 2006.
- [7] I. Volosyak, O. Ivlev, and A. Grser, "Rehabilitation robot friend ii—the general concept and current implementation," in *Proc. of the IEEE 9th Int. Conf. On Rehabilitation Robotics (ICORR 2005)*, 2005, pp. 540–544.
- [8] R. M. Mahoney, "The raptor wheelchair robot system," in *Integration of assistive technology in the information age: ICORR'2001, 7th International Conference on Rehabilitation Robotics*. Ios Pr Inc, 2001, p. 135.
- [9] H. Efring and K. Boschian, "Technical results from manus user trials," in *Proc. 6th Int. Conf. on Rehabilitation Robotics*, 1999, p. 136141.
- [10] K. Ikuta, H. Ishii, and M. Nokata, "Safety evaluation method of design and control for human-care robots," *The International Journal of Robotics Research*, vol. 22, no. 5, p. 281, 2003.
- [11] B. Brogliato, R. Ortega, and R. Lozano, "Global tracking controllers for flexible-joint manipulators: a comparative study," *AUTOMATICA-OXFORD-*, vol. 31, pp. 941–941, 1995.
- [12] M. Zinn, B. Roth, O. Khatib, and J. K. Salisbury, "A new actuation approach for human friendly robot design," *International Journal of Robotics Research*, vol. 23, no. 4, pp. 379–398, 2004.
- [13] T. Sugaiwa, H. Iwata, and S. Sugano, "New visco-elastic mechanism design for flexible joint manipulator," in *IEEE/ASME International Conference on Advanced Intelligent Mechatronics, 2008. AIM 2008*, 2008, pp. 235–240.
- [14] J. Pratt, B. Krupp, and C. Morse, "Series elastic actuators for high fidelity force control," *Industrial Robot: An International Journal*, vol. 29, no. 3, pp. 234–241, 2002.
- [15] D. W. Robinson, *Design and analysis of series elasticity in closed-loop actuator force control*, 2000.
- [16] H. Iwata, H. Hoshino, T. Morita, and S. Sugano, "A physical interference adapting hardware system using mia arm andhumanoid surface covers," in *1999 IEEE/RSJ International Conference on Intelligent Robots and Systems, 1999. IROS'99. Proceedings*, vol. 2, 1999.
- [17] A. Albu-Schaffer, C. Ott, and G. Hirzinger, "A unified passivity-based control framework for position, torque and impedance control of flexible joint robots," *The International Journal of Robotics Research*, vol. 26, no. 1, p. 23, 2007.
- [18] C. Ott, A. Albu-Schaffer, A. Kugi, and G. Hirzinger, "On the passivity-based impedance control of flexible joint robots," *IEEE Transactions on Robotics*, vol. 24, no. 2, pp. 416–429, 2008.
- [19] A. D. Luca, B. Siciliano, and L. Zollo, "Pd control with on-line gravity compensation for robots with elastic joints: Theory and experiments," *Automatica*, vol. 41, no. 10, pp. 1809–1819, 2005.
- [20] L. Zollo, B. Siciliano, A. D. Luca, E. Guglielmelli, and P. Dario, "Compliance control for an anthropomorphic robot with elastic joints: Theory and experiments," *Journal of Dynamic Systems, Measurement, and Control*, vol. 127, p. 321, 2005.
- [21] N. Ulrich and V. Kumar, "Passive mechanical gravity compensation for robot manipulators," in *1991 IEEE International Conference on Robotics and Automation, 1991. Proceedings.*, 1991, pp. 1536–1541.
- [22] Y. Ono and T. Morita, "A wiggling manipulator equipped with a mechanical gravity canceller (hyper performance robotics and mechatronics, session: Ta1-b)."